European Journal of Medicinal Chemistry 46 (2011) 383–392

Contents lists available at ScienceDirect

European Journal of Medicinal Chemistry

journal homepage: http://www.elsevier.com/locate/ejmech

Short communication

1,2,5-Oxadiazole analogues of leflunomide and related compounds

Marta Giorgis [a], Marco Lucio Lolli [a], Barbara Rolando [a], Angela Rao [a], Paolo Tosco [a], Shilpi Chaurasia [a], Domenica Marabello [b], Roberta Fruttero [a], Alberto Gasco [a,*]

[a] Dipartimento di Scienza e Tecnologia del Farmaco, Università di Torino, Via Pietro Giuria 9, I-10125 Torino, Italy
[b] Dipartimento di Chimica I.F.M. e Centro Interdipartimentale di Cristallografia Diffrattometrica CrisDi, Università di Torino, Via Pietro Giuria 7, I-10125 Torino, Italy

ARTICLE INFO

Article history:
Received 23 July 2010
Received in revised form
26 October 2010
Accepted 27 October 2010
Available online 3 November 2010

Keywords:
Cyano-oximes
Dihydroorotate dehydrogenase inhibitors
Furazans
Leflunomide

ABSTRACT

A new series of compounds, structurally related to leflunomide, based on the 1,2,5-oxadiazole ring system (furazan) has been synthesised, and their ability to undergo ring scission at physiological pH to afford the corresponding cyano-oximes has been analyzed. The latter, together with the respective nitro derivatives obtained by oxidation, have been characterised as weak inhibitors of rat dihydroorotate dehydrogenase (DHODH).

1. Introduction

Leflunomide **1** is a drug used in the treatment of rheumatoid arthritis [1]. It behaves as a prodrug, since its isoxazole heterocyclic system is rapidly transformed, upon absorption, into the active metabolite A771726, which was assigned the *Z*-configuration **1a** (Fig. 1) [2]. This transformation has been principally regarded as a non-enzymatic reaction, amenable to the capacity of 3-unsubstituted isoxazoles to undergo ring opening to nitrile enolates under mild basic conditions [3]. More recently, the possibility of heteroring scission catalyzed by cytochrome P-450 has also been taken into account [4]. This drug seems to exert its anti-inflammatory action through a number of mechanisms. In particular, it is able to inhibit *de novo* pyrimidine biosynthesis through blockade of dihydroorotate dehydrogenase (DHODH) [5] and to reduce the release of histamine from mast cells [6]. In addition, A771726 acts as inhibitor of tyrosine kinase [7]. Also 3-monosubstituted 1,2,5-oxadiazoles (furazans) (**1b**, Fig. 1) are quite sensitive to bases, which induce ring opening yielding α-oximinoacetonitrile derivatives (cyano-oximes) (**1c**, Fig. 1) [8–10]. In order to explore the potential bioisosterism between isoxazoles and furazans, we designed a series of compounds structurally related to leflunomide, containing the furazan ring (**3a**–**14a**, Scheme 1). In this paper, we report the synthesis of these compounds, their ability to undergo ring scission under different pH conditions to afford the corresponding cyano-oximes **3b**–**14b**, and the oxidation of selected cyano-oximes to the nitro derivatives **3c**–**10c**, **12c**, **14c** (Scheme 1). The ionization behaviour of the newly synthesised products as well as the results of their preliminary pharmacological characterization as inhibitors of rat DHODH are also discussed. A molecular modelling investigation was carried out to shed light on the biological activity profile obtained from in vitro assays.

2. Chemistry

The synthetic pathway used to prepare the products described in the present work is reported in Scheme 1. The *N*-substituted furazancarboxamides **3a**–**14a** were obtained by direct coupling in tetrahydrofuran (THF) solution of furazancarboxylic acid **2** with the appropriate anilines **3**–**14** in the presence of dichloro(triphenyl) phosphorane (Ph_3PCl_2). These compounds were converted into the corresponding oximes **3b**–**14b** by treatment with NaOH in methanol solution. $KMnO_4$ oxidation in acetone/water of a number of oxime derivatives afforded the nitro compounds **3c**-**10c**, **12c**, **14c**. ^1H and ^{13}C-NMR spectra are in keeping with the proposed structures. In particular, we assigned the *E* configuration to the oxime compounds on the basis of their ^{13}C-NMR spectra; for all these products the $^{13}C{\equiv}N$ chemical shifts fell in the very narrow range 108.6–109.6 ppm (DMSO-d_6). A similar chemical shift (109.66 ppm) was measured, in the same solvent, for the $^{13}C{\equiv}N$

* Corresponding author. Tel.: +39 0116707670; fax: +39 0116707286.
E-mail address: alberto.gasco@unito.it (A. Gasco).

0223-5234/$ – see front matter © 2010 Elsevier Masson SAS. All rights reserved.
doi:10.1016/j.ejmech.2010.10.029

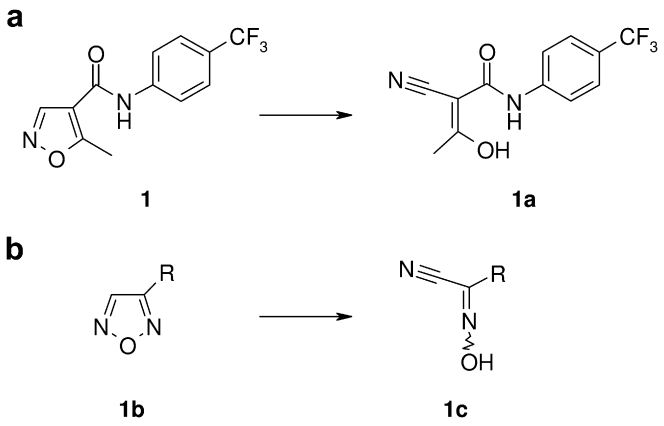

Fig. 1. Ring opening of leflunomide **1** to its active metabolite A771726 **1a** (a) and of a generic 3-monosubstituted furazan **1b** to the α-oximinoacetonitrile derivative **1c** (b).

group of the *E*-2-cyano-2-isonitroso-*N*-morpholinylacetamide (**A**, Fig. 2) [11]. When **A** was heated at 100 °C in DMSO-d_6, it underwent partial conversion into its *Z*-stereoisomer (**B**, Fig. 2), which showed the $^{13}C{\equiv}N$ resonance at 113.66 ppm. This is in keeping with the known shielding effect exerted by the oxime OH that induces an upfield shift on the adjacent carbon (steric compression shift) [12]. All the attempts to obtain thermal isomerisation under the same conditions of cyano-oximes described in the present work

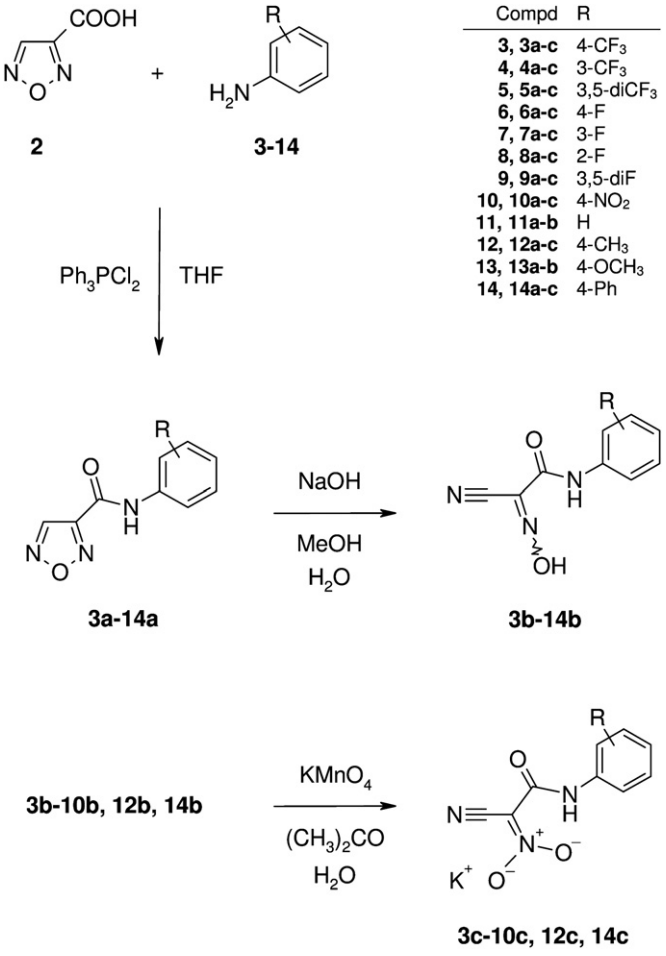

Scheme 1. Synthetic route to compounds object of this work.

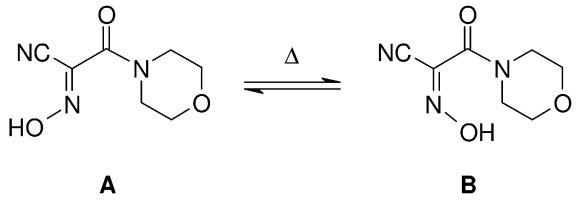

Fig. 2. *E*-2-cyano-2-isonitroso-*N*-morpholinylacetamide **A** and its partial thermal conversion to the *Z*-stereoisomer **B**.

failed. A similar behaviour had already been observed for some carbamoyl-substituted cyano-oximes [13]. Also the preparation of the oxime derivatives **3b**–**14b** by action of isopentylnitrite on the corresponding sodium salts of 2-cyano-*N*-phenylacetamides afforded only the *E* forms. A theoretical DFT study was carried out to compute the relative thermodynamic stabilities of *E* and *Z* isomers for compounds **3b**, **10b**, **14b**, which confirmed that the *E* isomer is consistently about 3.7 kcal mol^{-1} more stable (Table 1). For compound **3b** the minimum energy reaction path for the *E*-*Z* isomerisation was computed as previously described [14], finding an activation energy of 52.7 kcal mol^{-1} (Fig. 3), which is in excellent accordance with the one reported for (hydroxyimino)propanedinitrile (54.9 kcal mol^{-1}) [14]. Both the greater thermodynamic stability of the *E* isomer and the high energy barrier make isomerisation not viable under the experimental conditions described above.

2.1. X-ray diffraction

An X-ray diffraction study confirmed the assigned *E* configuration for compounds **6b**, **8b** (Fig. 4). Both molecules deviate from planarity and the phenyl ring is rotated around C(1)–N(1) by 17° in **6b** and by 23° in **8b** with respect to the nearly planar part of the molecule. The figure shows the *E* configuration with respect to the C(8)–N(2) double bond (1.277(6) and 1.279(1) Å for **6b** and **8b** respectively). All the C-N bond distances are in agreement with the values reported in literature for analogous bonds [15]. Also the C-C and C-O bond distances agree with literature values. The packing diagram of both structures shows two types of intermolecular hydrogen bonds: H(1)···N(3) (2.41–2.57 Å) and H(2)···O(1) (1.83 Å average).

2.2. Kinetics of furazan ring opening

Kinetics of ring scission (Scheme 2) of furazancarboxamides **3a**–**14a** were assessed in buffered solution at physiological pH (7.4) at 37 °C by monitoring the disappearance of compounds by reversed-phase high-performance liquid chromatography (RP-HPLC). The ring opening strictly followed first-order kinetics. The measured half-lives ($t_{1/2}$) fall in the range 69.0–123.4 min; all values are reported in Table 2, together with the data found for leflunomide **1**, taken as reference. After 24-h incubation under the same conditions, only 20% of **1a** was formed from **1**. The most stable product was the phenyl substituted term **11a**, and the less stable the 4-nitrophenyl derivative **10a**. The behaviour of leflunomide and its strict analogue **3a** was also studied at pH 1 and 10. After 6 h both compounds were unaltered in acidic medium, while in basic conditions ring opening was strongly accelerated ($t_{1/2} < 1$ min and $t_{1/2} = 70$ min for **3a** and leflunomide **1**, respectively). This picture is in keeping with the knowledge that the furazan system undergoes base-induced ring scission much faster than the isoxazole ring [9].

Table 1
Relative thermodynamic stabilities of *Z* isomer compared to *E* isomer for oximes **3b**, **10b**, **14b**.

Compd	$\Delta\Delta H_f$[a]
3b	3.69
10b	3.83
14b	3.58

[a] Relative stability of *Z* isomer compared to *E* isomer (kcal mol^{-1}); values represent the difference between the enthalpies of formation (ΔH_f) at 0 K.

2.3. Dissociation constants

Potentiometric titrations of the oxime compounds **3b**–**14b** were carried out with a Sirius GLpK_a automated potentiometric system. The titrations were performed in water using methanol in different ratios as co-solvent. The aqueous pK_as (Table 3) were determined by extrapolation to 0% methanol, according to the Yasuda–Shedlovsky procedure [16]. All the oximes behave as quite strong acids in accordance with the presence of two electron withdrawing groups on the hydroxyimino moiety. Their pK_a values fall in the range 4.61–5.12, the most acidic product being the 4-nitrophenyl substituted compound **10b**, the least acidic the phenyl substituted term **11b**. Consequently, as in the case of **1a**, the ionised forms are largely predominant for all the products at physiological pH. The determination of dissociation constants of all nitro derivatives by potentiometric titration was prevented by their marked acidity.

3. Results and discussion

DHODH (EC 1.3.99.11) is a mitochondrial protein involved in *de novo* pyrimidine biosynthesis. It catalyses the ubiquinone-mediated oxidation of dihydroorotate (DHO) to orotate [17]. DHODH is considered as an important target for the development of immunomodulating agents. A771726 **1a** is a potent inhibitor of this enzyme. The *Z* configuration of **1a** bears the enolic hydroxy group in *cis* position with respect to the amide moiety. The experimental binding mode of this configuration within the active site of human DHODH has been reported [18]. In particular, the 4-trifluoromethylphenyl moiety establishes several hydrophobic contacts with residues of the tunnel leading to active site. The enolic OH group interacts via hydrogen bonding with Tyr356, while the amide carbonyl is hydrogen bonded to Arg136 through a water molecule. SAR studies carried out on analogues of A771726 show that the most potent inhibitors contain a cyclopropyl residue at the 3-position of the 3-hydroxy propenamide scaffold, while larger substituents are detrimental to the activity. In addition, they bear at the 4-position of the phenyl ring small lipophilic groups, as well as weak hydrogen bond acceptors [19]. In view of the quick conversion at physiological pH of furazans **3a**–**14a** into the related oxime derivatives **3b**–**14b**, only these latter compounds and some of their nitro counterparts were assayed for their DHODH inhibitory potency on rat liver mithocondrial/microsomal membranes. A procedure adapted from literature was employed, in which oxidation of DHO to orotate is monitored following the concomitant reduction of the chromophore 2,6-dichlorophenolindophenol (DCIP) [20]; the results are collected in Table 3. Analysis of the data shows that most products are inactive when tested at 100 μM. 4-Fluorophenyl and 3,5-difluorophenyl substituted compounds **6b** and **9b** at this concentration were able to trigger feeble inhibition of the enzyme, 27% and 23%, respectively. Only the strict oxime

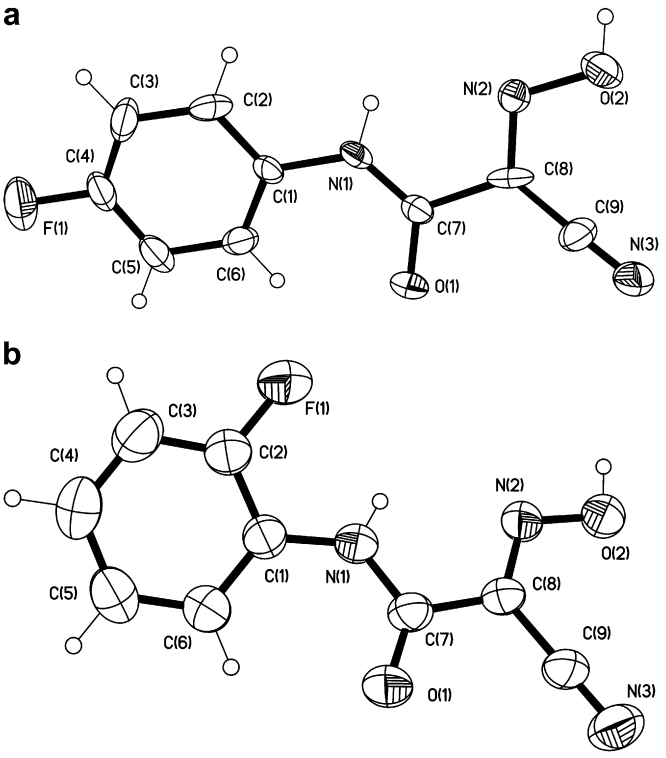

Fig. 4. ORTEP plot (30% of probability) of one of the two **6b** molecules of the asymmetric unit (a) and ORTEP plot (50% of probability) of **8b** (b).

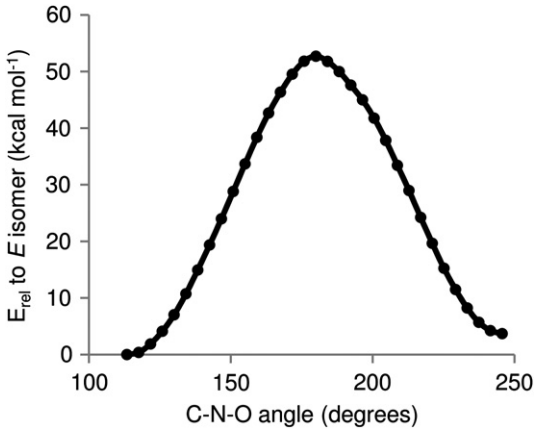

Fig. 3. Minimum energy reaction path for the *E-Z* isomerisation of oxime **3b**. Total molecular energies are reported relative to the ground state energy of isomer *E*.

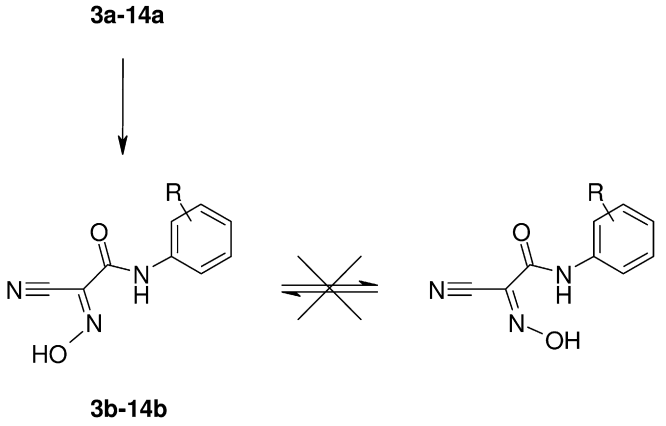

Scheme 2. Ring scission of furazancarboxamides **3a**–**14a**.

Table 2
Stability of leflunomide **1** and furazan derivatives **3a**–**14a** in buffered solution (pH = 7.4).

Compd	$t_{1/2}$[a]
1	ND[b]
3a	82.5
4a	100.7
5a	90.9
6a	88.7
7a	108.5
8a	102.2
9a	92.0
10a	69.0
11a	123.4
12a	113.4
13a	106.4
14a	76.9

[a] Half-life (min) calculated by fitting with first-order decay function; SE < 0.6.
[b] Half-life >24 h (80% of unchanged compound after 24 h).

analogue of A771726 **3b** was able to inhibit the enzyme in a concentration-dependent manner ($IC_{50} = 60$ μM), although much less effectively than the lead. The general very low inhibitory activity of these products could be ascribed to the *E* configuration of the oxime group, which prevents them from assuming the same binding mode of the lead in the active cleft of the enzyme. Also the nitro substituted compounds **3c**–**10c**, **12c**, **14c** are not potent inhibitors, but overall more effective than the corresponding oximes. The most potent product was **3c**, the strict analogue of A771726, followed by the 4-phenyl and 4-nitro substituted products **14c** and **10c**, respectively. All the other terms of the series

Table 3
Dissociation constants of oxime derivatives **3b**–**14b** and inhibition of rat liver DHODH activity by reference compounds **1** and **1a**, oxime derivatives **3b**–**14b** and nitro compounds **3c**-**10c**, **12c**, **14c**.

Compd	$pK_a \pm SD$[a]	DHODH inhibition	
		$IC_{50} \pm SE$ [μM][b]	% inhibition ± SE[c]
1	-	1.6 ± 0.3	-
1a	-	0.020 ± 0.002	-
3b	4.87 ± 0.01	60 ± 18	-
4b	4.88 ± 0.02	-	-[d]
5b	4.73 ± 0.01	-	-[d]
6b	5.01 ± 0.01	-	27 ± 5
7b	4.92 ± 0.01	-	-[d]
8b	4.87 ± 0.01	-	-[d]
9b	4.81 ± 0.01	-	23 ± 8
10b	4.61 ± 0.01	-	-[d]
11b	5.12 ± 0.02	-	-[d]
12b	5.07 ± 0.01	-	-[d]
13b	5.08 ± 0.01	-	-[d]
14b	5.03 ± 0.01	-	-[d]
3c	-	17 ± 2	-
4c	-	-	29 ± 2
5c	-	-	21 ± 4
6c	-	-	24 ± 5
7c	-	-	26 ± 2
8c	-	-	22 ± 4
9c	-	-	22 ± 2
10c	-	74 ± 6	-
12c	-	-	20 ± 3
14c	-	26 ± 4	-

[a] Determined by potentiometry; MeOH was used as cosolvent in percentage ranging from 24 to 58 (%wt); the extrapolation to zero was obtained by the Yasuda–Shedlovsky procedure [16].
[b] Enzyme activity was measured by DCIP reduction assay and IC_{50} values were calculated with non-linear regression analysis.
[c] Enzyme activity was measured by DCIP reduction assay and % of inhibition at the highest tested concentration (100 μM) was reported.
[d] Compound was inactive at 100 μM.

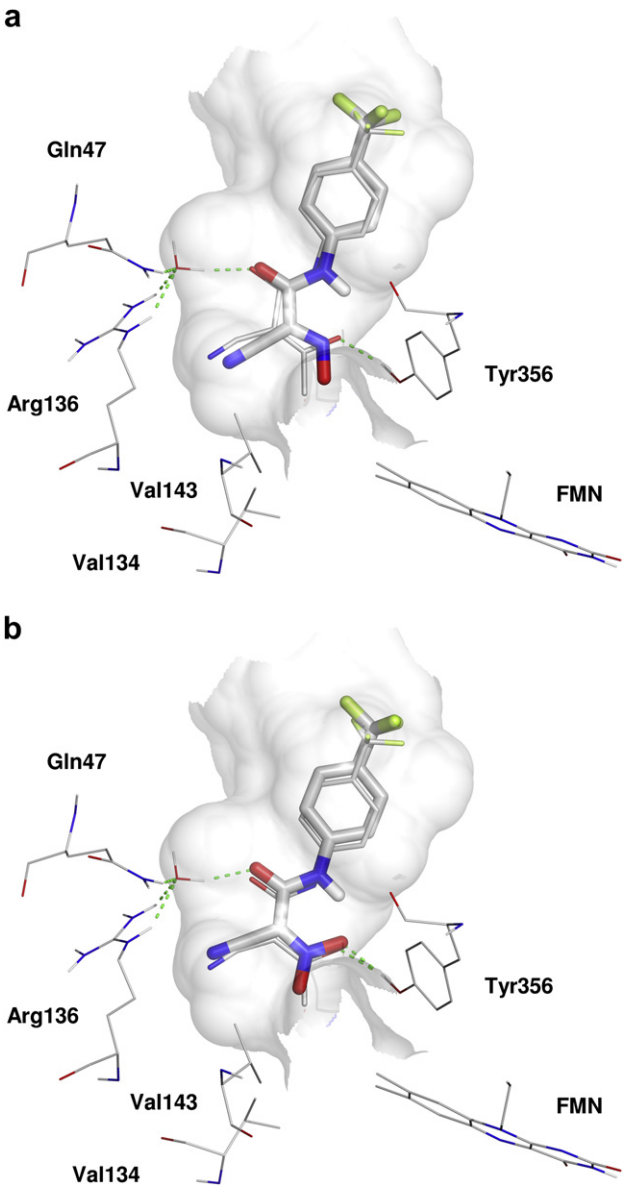

Fig. 5. Interactions of **3b** (a) and **3c** (b) with human DHODH in the inhibitor's binding site; the pose of co-crystallized **1a** (thinner sticks) is also reported as a reference.

inhibited the activity of the enzyme only to the extent of 20–29%, when tested at 100 μM. Docking of the most active compounds into the active site of DHODH confirmed the inability of oximes to hydrogen bond to Tyr356 due to their inappropriate stereochemistry (Fig. 5a). While nitro compounds have the correct geometry to interact productively with Tyr356, on one side the charge-enhanced hydrogen bond is not as strong as for the leflunomide metabolite **1a** since the negative charge is spread on two oxygen atoms instead of being mostly localized on the enolic oxygen. On the other side, the other negatively charged oxygen does not interact as effectively as leflunomide's methyl group with the lipophilic pocket delimited by Val134, Val143 and the two methyl groups of flavin mononucleotide (FMN) (Fig. 5b). These considerations provide a rationale for the lower activity of the newly synthesised analogues compared to the lead. Both the human DHODH in complex with leflunomide [18] and rat DHODH in complex with brequinar [21] were used as docking targets obtaining the same results, proving that the small differences in terms of primary and

tertiary structure between the two isozymes do not influence the binding mode of the compounds object of this work.

4. Conclusions

A series of furazan analogues of leflunomide have been realised (**3a**–**14a**). These compounds are readily converted at physiological pH into their oxime counterparts (**3b**–**14b**). The latter have been assayed as DHODH inhibitors; their low potency is probably due to the unfavourable stereochemistry of the oxime substructure, which cannot effectively mimic the enolate moiety of A771726. Oxidation of the oxime group to nitro improved the activity on DHODH, putting into evidence the importance of a properly oriented charge-enhanced hydrogen bond acceptor. Further efforts are ongoing to obtain more potent leflunomide bioisosters.

5. Experimental protocols

5.1. Chemistry

Melting points were determined on a Büchi 530 apparatus. The compounds were routinely checked by IR spectroscopy (Shimadzu, FT-IR 8101 M) and mass spectrometry (Finnigan-Mat TSQ-700 spectrometer, 70 eV, direct inlet). ^{1}H and proton decoupled ^{13}C-NMR spectra were recorded on a Bruker AC-300 spectrometer. The following abbreviations are used: *s*, singlet; *d*, doublet; *q*, quartet; *m*, multiplet; Fz, furazan; PE, petroleum ether (40–60). Flash column chromatography was performed on silica gel (Merck Kieselgel 60, 230–400 mesh ASTM) using the indicated eluents. Thin layer chromatography (TLC) was carried out on 5-20 cm plates with a layer thickness of 0.25 mm; when necessary they were developed with iodine and $KMnO_4$. Anhydrous magnesium sulphate was used as drying agent of the organic extracts. THF was distilled immediately before use from sodium and benzophenone under N_2. Compounds **1** [22], **1a** [22] and **2** [23] were synthesised according to literature methods. Elemental analyses of the new compounds are within ±0.4% of the theoretical values and are reported in the Supplementary Material. In case of compounds **3c**, **5c** and **9c**, that showed elemental analyses slightly out of the commonly accepted range, the purity was also assessed by RP-HPLC (>99%). Analyses were performed on a HP1100 chromatograph system (Agilent Technologies, Palo Alto, CA, USA) equipped with an injector (Rheodyne, Cotati, CA, USA), a quaternary pump (model G1311A), a membrane degasser (model G1379A), and a diode-array detector (DAD, model G1315B) integrated in the HP1100 system. Data analysis was performed using a HP ChemStation system (Agilent Technologies). The analytical column was a Nucleosil 100-5C18 Nautilus (250 × 4.6 mm, 5 mm particle size) (Macherey-Nagel). Compounds were dissolved in CH_3CN and injected through a 20 μL loop. The mobile phase consisted of CH_3CN/water with 0.1% trifluoroacetic acid (ranging from 60/40 to 80/20 ratio, according to the retention factor of the compounds). HPLC retention times (t_R) were obtained at flow rates of 1.2 mL min^{-1}, and the column effluent was monitored at 210 and 270 nm referenced against 360 nm.

5.1.1. Furazancarboxamide derivatives: general synthetic procedure

To a stirred solution of furazancarboxylic acid **2** (2.6 mmol) and the appropriate aniline **3**–**14** (2.6 mmol) in dry THF (25 mL) Ph_3PCl_2 (5.46 mmol, 2.1 eq) was added portionwise under an inert atmosphere. The resulting suspension was stirred for 2 h, then poured into chilled 2 M HCl (50 mL). The mixture was extracted exhaustively with Et_2O, then the collected organic layers were dried and concentrated under reduced pressure. The residue was purified by flash chromatography obtaining the title compound.

5.1.1.1. N-[4-(Trifluoromethyl)phenyl]furazancarboxamide (**3a**).

White solid, flash chromatography eluent: PE/EtOAc 9:1 v/v; yield 40%; m.p. 145 °C (triturated with hexane); ^{1}H-NMR (DMSO-d_6): δ 7.77–8.03 (m, 4H, aromatic protons), 9.46 (s, 1H, FzC*H*), 11.43 (s, 1H, N*H*); ^{13}C-NMR (DMSO-d_6): δ 119.8, 124.1 (q, *C*F$_3$, $^1J_{CF}$ 271.7 Hz), 124.7 (q, *C* (4), $^2J_{CF}$ 32.1 Hz), 126.1 (q, *C*(3), $^3J_{CF}$ 3.9 Hz), 141.3 (q, *C*(2), $^4J_{CF}$ 1.3 Hz), 142.6, 151.4, 155.2; MS (CI) *m*/*z* 258 (M + 1)$^+$. Anal. ($C_{10}H_6F_3N_3O_2$) C, H, N.

5.1.1.2. N-[3-(Trifluoromethyl)phenyl]furazancarboxamide (**4a**).

White solid; yield 57%; m.p. 46–47 °C (twice purified by flash chromatography; eluents: PE/EtOAc 7:3 v/v, then PE/EtOAc/CH_2Cl_2 95:5:50 v/v/v); ^{1}H-NMR (DMSO-d_6): δ 7.54–8.24 (m, 4H, aromatic protons), 9.45 (s, 1H, FzC*H*), 11.40 (s, 1H, N*H*); ^{13}C-NMR (DMSO-d_6): δ 116.7 (q, *C*(4), $^3J_{CF}$ 4.2 Hz), 121.12 (q, *C*(2), $^3J_{CF}$ 3.8 Hz), 123.9 (q, *C*F$_3$, $^1J_{CF}$ 272.2 Hz), 124.1 (m, *C*(5)), 129.5 (q, *C*(3), $^2J_{CF}$ 31.7 Hz), 130.15, 138.5, 151.4, 155.1; MS (CI) *m*/*z* 258 (M + 1)$^+$. Anal. ($C_{10}H_6F_3N_3O_2$) C, H, N.

5.1.1.3. N-[3,5-Bis(trifluoromethyl)phenyl]furazancarboxamide (**5a**).

White solid; flash chromatography eluent: PE/EtOAc 7:3 v/v; yield 37%; m.p. 117–118 °C (from hexane/diethylether 1:1 v/v); ^{1}H-NMR (DMSO-d_6): δ 7.91 (s, 1H, C(4)*H*), 8.45 (s, 2H, C(2)*H*), 9.48 (s, 1H, N*H*), 11.70 (s, 1H, FzC*H*); ^{13}C-NMR (DMSO-d_6): δ 117.5–117.8 (m, *C*(4)), 120.2–120.5 (m, *C*(2)), 123.8 (q, *C*F$_3$, $^1J_{CF}$ 272.7 Hz), 130.8 (q, *C*(3), $^2J_{CF}$ 33.0 Hz), 139.7, 142.6, 151.2, 155.5; MS (CI) *m*/*z* 326 (M + 1)$^+$. Anal. ($C_{11}H_5F_6N_3O_2$) C, H, N.

5.1.1.4. N-(4-Fluorophenyl)furazancarboxamide (**6a**).

White solid; flash chromatography eluent: PE/EtOAc 7:3 v/v; yield 64%; m.p. 101 °C dec.(triturated with hexane/*i*Pr$_2$O); ^{1}H-NMR (DMSO-d_6): δ 7.22–7.82 (m, 4H, aromatic protons), 9.43 (s, 1H, FzC*H*), 11.16 (br s, 1H, N*H*); ^{13}C-NMR (DMSO-d_6): δ 116.5 (d, *C*(3), $^2J_{CF}$ 22.8 Hz), 124.1 (d, *C*(2), $^3J_{CF}$ 8.05 Hz), 135.0 (d, *C*(1), $^4J_{CF}$ 2.9 Hz), 142.8, 152.8, 156.7, 161.4 (d, *C*(4), $^1J_{CF}$ 243.3 Hz); MS (CI) *m*/*z* 208 (M + 1)$^+$. Anal. ($C_9H_6FN_3O_2$) C, H, N.

5.1.1.5. N-(3-Fluorophenyl)furazancarboxamide (**7a**).

White solid; flash chromatography eluent: PE/EtOAc 7:3 v/v; yield 57%; m.p. 109 °C (from hexane/diethylether); ^{1}H-NMR (DMSO-d_6): δ 7.00–7.74 (m, 4H, aromatic protons), 9.43 (s, 1H, FzC*H*), 11.29 (br s, 1H, N*H*); ^{13}C-NMR (DMSO-d_6): δ 109.1 (d, *C*(4), $^2J_{CF}$ 26.7 Hz), 112.7 (d, *C*(2), $^2J_{CF}$ 21.5 Hz), 117.4 (d, *C*(6), $^4J_{CF}$ 3.0 Hz), 131.4 (d, *C*(5), $^3J_{CF}$ 9.3 Hz), 140.6 (d, *C*(1), $^3J_{CF}$ 10.8 Hz), 142.8, 152.8, 156.8, 164.3 (d, *C* (3), $^1J_{CF}$ 243.2 Hz); MS (CI) *m*/*z* 208 (M + 1)$^+$. Anal. ($C_9H_6FN_3O_2$) C, H, N.

5.1.1.6. N-(2-Fluorophenyl)furazancarboxamide (**8a**).

White solid; flash chromatography eluent: PE/EtOAc 7:3 v/v; yield 37%; m.p. 81 °C (from hexane/isopropyl ether 1:1 v/v); ^{1}H-NMR (DMSO-d_6): δ 7.24–7.76 (m, 4H, aromatic protons), 9.45 (s, 1H, FzC*H*), 10.96 (br s, 1H, N*H*), ^{13}C-NMR (DMSO-d_6): δ 115.9 (d, *C*(3), $^2J_{CF}$ 19.6 Hz), 123.8 (d, *C*(1), $^2J_{CF}$ 12.3 Hz), 124.4 (d, *C*(4), $^3J_{CF}$ 3.6 Hz), 126.7 (d, *C*(5), $^4J_{CF}$ 1.40 Hz), 127.8 (d, *C*(6), $^3J_{CF}$ 7.9 Hz), 142.3, 150.9, 154.9, 155.4 (d, *C*(2), $^1J_{CF}$ 248.1 Hz); MS (CI) *m*/*z* 208 (M + 1)$^+$. Anal. ($C_9H_6FN_3O_2$) C, H, N.

5.1.1.7. N-(3,5-Difluorophenyl)furazancarboxamide (**9a**).

White solid; flash chromatography eluent: PE/EtOAc 7:3 v/v; yield 53%; m.p. 112–113 °C (from hexane/diethylether 1:1 v/v); ^{1}H-NMR (DMSO-d_6): δ 7.04–7.60 (m, 3H, aromatic protons), 9.45 (s, 1H, N*H*), 11.45 (s, 1H, FzC*H*); ^{13}C-NMR (DMSO-d_6): δ 100.7 (t, *C*(4), $^2J_{CF}$ 26.1 Hz), 104.7 (m, *C*(2)), 141.4 (t, *C*(1), $^3J_{CF}$ 13.6 Hz), 142.8, 152.6, 156.9, 164.5 (dd, *C*(3), $^1J_{CF}$ 244.9 Hz, $^3J_{CF}$ 14.6 Hz); MS (CI) *m*/*z* 226 (M + 1)$^+$. Anal. ($C_9H_5F_2N_3O_2$) C, H, N.

*5.1.1.8. N-(4-Nitrophenyl)furazancarboxamide (**10a**).* White solid; flash chromatography eluent: PE/EtOAc 8:2 v/v; yield 25%; m.p. 266.9–267.1 °C dec. (from hexane/isopropyl ether 1:1 v/v); ^{1}H-NMR (DMSO-d_6): δ 8.05–8.32 (m, 4H, aromatic protons), 9.47 (s, 1H, N*H*), 11.62 (s, 1H, FzC*H*); ^{13}C-NMR (DMSO-d_6): δ 124.8, 142.6, 143.3, 143.8, 151.3, 155.4, 157.6; MS (CI) *m*/*z* 235 $(M+1)^+$. Anal. ($C_9H_6N_4O_4$) C, H, N.

*5.1.1.9. N-Phenylfurazancarboxamide (**11a**).* Pale yellow solid; flash chromatography eluent: PE/EtOAc 6:4 v/v; yield 34%; m.p. 138 °C (from hexane/isopropyl ether 9:1 v/v); ^{1}H-NMR (DMSO-d_6): δ 7.16–7.79 (m, 5H, aromatic protons), 9.43 (s, 1H, FzC*H*), 11.08 (br s, 1H, N*H*); ^{13}C-NMR (DMSO-d_6): δ 121.4, 125.7, 129.7, 138.6, 143.4, 152.5, 155.6; MS (CI) *m*/*z* 190 $(M+1)^+$. Anal. ($C_9H_7N_3O_2 \cdot 0.1H_2O$) C, H, N.

*5.1.1.10. N-(4-Methylphenyl)furazancarboxamide (**12a**).* White solid; flash chromatography eluent: PE/EtOAc 7:3 v/v; yield 46%; m.p. 138 °C (from hexane/isopropyl ether 1:1 v/v); ^{1}H-NMR (DMSO-d_6): δ 3.33 (s, 3H, CH_3), 7.19–7.66 (m, 4H, aromatic protons), 9.40 (s, 1H, N*H*), 10.99 (s, 1H, FzC*H*); ^{13}C-NMR (DMSO-d_6): δ 21.1, 122.2, 130.5, 136.2, 136.3, 142.8, 153.0, 156.6; MS (CI) *m*/*z* 204 $(M+1)^+$. Anal. ($C_{10}H_9N_3O_2$) C, H, N.

*5.1.1.11. N-(4-Methoxyphenyl)furazancarboxamide (**13a**).* Pale gray solid; flash chromatography eluent: PE/EtOAc 7:3 v/v; yield 62%; m.p. 131 °C (from hexane/isopropyl ether 1:1 v/v); ^{1}H-NMR (DMSO-d_6): δ 3.76 (s, 3H, OCH_3), 6.96–7.71 (m, 4H, aromatic protons), 9.40 (s, 1H, N*H*), 10.96 (s, 1H, FzC*H*); ^{13}C-NMR (DMSO-d_6): δ 55.1, 113.9, 122.1, 130.6, 142.4, 151.6, 154.2, 156.2; MS (CI) *m*/*z* 220 $(M+1)^+$. Anal. ($C_{10}H_9N_3O_3$) C, H, N.

*5.1.1.12. N-(Biphenyl-4-yl)furazancarboxamide (**14a**).* Yellow solid; flash chromatography eluent: PE/EtOAc 7:3 v/v; yield 39%; m.p. 199 °C (from hexane/isopropyl ether 1:1 v/v); ^{1}H-NMR (DMSO-d_6): δ 9.79 (s, 1H, FzC*H*), 7.33–7.90 (m, 9H, aromatic protons), 11.20 (br s, 1H, N*H*); ^{13}C-NMR (DMSO-d_6): δ 122.0, 127.4, 128.0, 128.1, 129.7, 138.0, 138.4, 141.0, 142.8, 152.6, 155.9; MS (CI) *m*/*z* 266 $(M+1)^+$. Anal. ($C_{15}H_{11}N_3O_2$) C, H, N.

5.1.2. 2-Hydroxyiminopropionitrile derivatives: general synthetic procedure

1 M NaOH (4.2 mmol, 4.2 mL) was added to an ice-cooled solution of the amide **3a**–**13a** (1 mmol) in MeOH (11 mL). The mixture was stirred at room temperature for 2 h, then diluted with water (5 mL). The pH of the mixture was adjusted to 1 by addition of 6 M HCl. The resulting suspension was exhaustively extracted with Et_2O. The organic layers were collected, dried and concentrated under reduced pressure to afford the pure title compound.

*5.1.2.1. 2-Hydroxyimino-3-oxo-3-[4-(trifluoromethyl)phenyl]amino-propionitrile (**3b**).* White solid; yield 89%; m.p. 210–211 °C (from toluene); ^{1}H-NMR (DMSO-d_6): δ 7.72–7.96 (m, 4H, aromatic protons), 10.78 (s, 1H, N*H*), 14.76 (br s, 1H, O*H*); ^{13}C-NMR (CD_3OD): δ 108.7, 120.6, 124.1 (q, *C*F$_3$, $^1J_{CF}$ 271.7 Hz), 124.3 (q, *C*(4), $^2J_{CF}$ 32.0 Hz), 125.9 (q, *C*(3), $^3J_{CF}$ 3.8 Hz), 141.2 (q, *C*(2), $^4J_{CF}$ 1.4 Hz), 157.3; MS (CI) *m*/*z* 258 $(M+1)^+$. Anal. ($C_{10}H_6F_3N_3O_2$) C, H, N.

*5.1.2.2. 2-Hydroxyimino-3-oxo-3-[3-(trifluoromethyl)phenyl]amino-propionitrile (**4b**).* White solid; yield 74%; m.p. 181 °C (from toluene); ^{1}H-NMR (DMSO-d_6): δ 7.49–8.16 (m, 4H, aromatic protons), 10.75 (br s, 1H, N*H*), 14.78 (br s, 1H, O*H*); ^{13}C-NMR (DMSO-d_6): δ 109.6, 117.8 (q, *C*(4), $^3J_{CF}$ 4.2 Hz), 121.7 (q, *C*(2), $^3J_{CF}$ 3.8 Hz), 124.9 (q, *C*F$_3$, $^1J_{CF}$ 272.3 Hz), 125.2–125.3 (m), 129.3, 130.3 (q, *C*(3), $^2J_{CF}$ 31.8 Hz), 130.8, 139.3, 158.3; MS (CI) *m*/*z* 258 $(M+1)^+$. Anal. ($C_{10}H_6F_3N_3O_2$) C, H, N.

*5.1.2.3. 3-[3,5-Bis(trifluoromethyl)phenyl]amino-2-hydroxyimino-3-oxopropionitrile (**5b**).* White solid; yield 98%; m.p. 191 °C dec. (from toluene); ^{1}H-NMR (DMSO-d_6): δ 7.85 (s, 2H, C(2)*H*), 8.45 (s, 2H, C(2)*H*), 11.03 (s, 1H, N*H*), 14.89 (s, 1H, O*H*); ^{13}C-NMR (DMSO-d_6): δ 108.6, 117.2–117.3 (m, *C*(4)), 120.4–120.6 (m, *C*(2)), 123.8 (q, *C*F$_3$, $^1J_{CF}$ 272.7 Hz), 128.3, 130.8 (q, *C*(3), $^2J_{CF}$ 32.9 Hz), 139.7, 157.8; MS (CI) *m*/*z* 326 $(M+1)^+$. Anal. ($C_{11}H_5F_6N_3O_2$) C, H, N.

*5.1.2.4. 3-(4-Fluorophenyl)amino-2-hydroxyimino-3-oxopropionitrile (**6b**).* Pale yellow; yield 78%; m.p. 184 °C dec. (triturated with toluene); ^{1}H-NMR (DMSO-d_6): δ 7.17–7.63 (m, 4H, aromatic protons), 14.65 (br s, 1H, O*H*), 10.49 (br s, 1H, N*H*); ^{13}C-NMR (DMSO-d_6): δ 109.1, 116.4 (d, *C*(3), $^2J_{CF}$ 22.8 Hz), 124.1 (d, *C*(2), $^3J_{CF}$ 8.0 Hz), 129.8, 134.8 (d, *C*(1), $^4J_{CF}$ 2.9 Hz), 158.8, 161.2 (d, *C*(4), $^1J_{CF}$ 243.0 Hz); MS (CI) *m*/*z* 208 $(M+1)^+$. Anal. ($C_9H_6FN_3O_2$) C, H, N.

*5.1.2.5. 3-(3-Fluorophenyl)amino-2-hydroxyimino-3-oxopropionitrile (**7b**).* White solid; yield 86%; m.p. 190 °C (from toluene); ^{1}H-NMR (DMSO-d_6): δ 6.94–7.65 (m, 4H, aromatic protons), 14.71 (s, 1H, O*H*), 10.61 (s, 1H, N*H*); ^{13}C-NMR (DMSO-d_6): δ 108.9, 108.9 (d, *C*(4), $^2J_{CF}$ 26.6 Hz), 112.4 (d, *C*(2), $^2J_{CF}$ 21.5 Hz), 117.4 (d, *C*(6), $^4J_{CF}$ 3.0 Hz), 131.3 (d, *C*(5), $^3J_{CF}$ 9.3 Hz), 140.9 (d, *C*(1), $^3J_{CF}$ 10.9 Hz), 129.8, 158.7, 164.2 (d, *C*(3), $^1J_{CF}$ 243.1 Hz); MS (EI) *m*/*z* 207 $(M)^+$. Anal. ($C_9H_6FN_3O_2$) C, H, N.

*5.1.2.6. 3-(2-Fluorophenyl)amino-2-hydroxyimino-3-oxopropionitrile (**8b**).* White solid, yield 99%; m.p. 198 °C dec. (from toluene); ^{1}H-NMR (DMSO-d_6): δ 7.20–7.64 (m, 4H, aromatic protons), 10.11 (s, 1H, N*H*), 14.82 (s, 1H, O*H*); ^{13}C-NMR (DMSO-d_6): δ 108.6, 115.8 (*d*, *C*(3), $^2J_{CF}$ 19.6 Hz), 124.1 (*d*, *C*(1), $^2J_{CF}$ 12.0 Hz), 124.4 (*d*, *C*(4), $^3J_{CF}$ 3.7 Hz), 126.5 (*d*, *C*(5), $^4J_{CF}$ 1.3 Hz), 127.5 (*d*, *C*(6), $^3J_{CF}$ 7.9 Hz), 127.8, 155.4 (*d*, *C*(2), $^1J_{CF}$ 247.3 Hz), 156.9; MS (CI) *m*/*z* 208 $(M+1)^+$. Anal. ($C_9H_6FN_3O_2$) C, H, N.

*5.1.2.7. 3-(3,5-Difluorophenyl)amino-2-hydroxyimino-3-oxopropionitrile (**9b**).* White solid; yield 89%; m.p. 202 °C dec. (from toluene); ^{1}H-NMR (DMSO-d_6): δ 6.98–7.53 (m, 4H, aromatic protons), 10.76 (s, 1H, N*H*), 14.78 (s, 1H, O*H*); ^{13}C-NMR (DMSO-d_6): δ 100.7 (t, *C*(4), $^2J_{CF}$ 26.1 Hz), 104.4–104.8 (m, *C*(2)), 108.8, 129.7, 141.4 (t, *C*(1), $^3J_{CF}$ 13.5 Hz), 158.9, 164.5 (dd, *C*(3), $^1J_{CF}$ 244.9 Hz, $^3J_{CF}$ 14.7 Hz); MS (CI) *m*/*z* 226 $(M+1)^+$. Anal. ($C_9H_5F_2N_3O_2$) C, H, N.

*5.1.2.8. 2-Hydroxyimino-3-(4-nitrophenyl)amino-3-oxopropionitrile (**10b**).* Pale yellow solid; yield 83%; m.p. 273.6–274.5 °C dec. (from toluene); ^{1}H-NMR (DMSO-d_6): δ 7.96–8.29 (m 4H, aromatic protons), 10.99 (br s, 1H, N*H*), 14.84 (br s, 1H, O*H*); ^{13}C-NMR (DMSO-d_6): δ 108.6, 120.4, 124.7, 128.4, 143.0, 143.8, 157.6; MS (CI) *m*/*z* 235 $(M+1)^+$. Anal. ($C_9H_6N_4O_4 \cdot 0.1\ H_2O$) C, H, N.

*5.1.2.9. 2-Hydroxyimino-3-oxo-3-phenylaminopropionitrile (**11b**).* Pale yellow solid; yield 91%; m.p. 202.2–202.7 °C dec. (triturated with toluene; lit 229–230 °C [24]); ^{1}H-NMR (DMSO-d_6): δ 7.12–7.71 (m, 5H, aromatic protons), 10.43 (s, 1H, N*H*), 14.66 (br s, 1H, O*H*); ^{13}C-NMR (DMSO-d_6): δ 108.8, 120.7, 124.5, 128.5, 128.6, 137.5, 156.7; MS (CI) *m*/*z* 190 $(M+1)^+$. Anal. ($C_9H_7N_3O_2$) C, H, N.

*5.1.2.10. 2-Hydroxyimino-3-(4-methylphenyl)amino-3-oxopropionitrile (**12b**).* Yellow solid; yield 94%; m.p. 238 °C (from toluene; lit 242–244 °C [24]); ^{1}H-NMR (DMSO-d_6) δ 2.27 (s, 3H, CH_3), 7.14–7.58 (m, 4H, aromatic protons), 10.35 (s, 1H, N*H*), 14.61 (br s, 1H, O*H*); ^{13}C-NMR (DMSO-d_6): δ 20.4, 108.8, 120.6, 128.5, 129.0, 133.3, 134.9, 156.5; MS (CI) *m*/*z* 204 $(M+1)^+$. Anal. ($C_{10}H_9N_3O_2$) C, H, N.

*5.1.2.11. 2-Hydroxyimino-3-(4-methoxyphenyl)amino-3-oxopropionitrile (**13b**).* Yellow solid; yield 81%; m.p. 221 °C (from toluene; lit

216–218 °C [24]); ^{1}H-NMR (DMSO-d_6): δ 3.74 (*s*, 3H, OC*H*$_3$), 6.91–7.61 (m, 4H, aromatic protons), 10.32 (*s*, 1H, N*H*), 14.58 (br s, 1H, O*H*); ^{13}C-NMR (DMSO-d_6): δ 55.1, 108.8, 113.7, 122.3, 128.5, 130.4, 156.0, 156.4; MS (CI) *m*/*z* 220 $(M+1)^+$. Anal. ($C_{10}H_9N_3O_3$) C, H, N.

*5.1.2.12. 2-Hydroxyimino-3-oxo-3-(biphenyl-4-yl)aminopropionitrile (**14b**).* Yellow solid; yield 80%; m.p. 250–251 °C (from toluene); ^{1}H-NMR (DMSO-d_6) δ 7.33–7.82 (m, 9H, aromatic protons), 10.55 (s, 1H, N*H*), 14.68 (br s, 1H, O*H*); ^{13}C-NMR (DMSO-d_6): δ 108.8, 121.0, 126.3, 126.8, 127.2, 128.6, 128.8, 136.1, 137.0, 139.4, 156.8; MS (CI) *m*/*z* 266 $(M+1)^+$. Anal. ($C_{15}H_{11}N_3O_2 \cdot 0.15H_2O$) C, H, N.

5.1.3. 2-Nitropropionitrile derivatives: general procedure

$KMnO_4$ (1.5 mmol, 237 mg) was added portionwise to an ice-cooled solution of the oxime (1.0 mmol) in acetone/water (1:2 v/v; 20 mL). The mixture was stirred at room temperature for 24 h, then filtered under Celite. The filtrate was acidified to pH 3 by adding glacial CH_3COOH, then washed with Et_2O (2 × 20 mL), and concentrated under reduced pressure. The resulting solid was triturated with isopropyl ether obtaining the title compound as potassium salt.

*5.1.3.1. 2-Nitro-3-oxo-3-[(4-trifluoromethyl)phenyl]aminopropionitrile potassium salt (**3c**).* White solid; yield 80%; m.p. 256.0–256.3 °C dec. (triturated with *i*Pr_2O); ^{1}H-NMR (DMSO-d_6): δ 7.65–7.82 (m, 4H, aromatic protons), 11.43 (s, 1H, N*H*); ^{13}C-NMR (DMSO-d_6): δ 98.4, 124.4 (q, *C*F$_3$, $^1J_{CF}$ 271.9 Hz), 124.7 (q, *C*(4), $^2J_{CF}$ 32.4 Hz), 126.0 (q, *C*(3), $^3J_{CF}$ 3.1 Hz), 129.8, 142.2 (m, *C*(2)), 160.3 (br s, NC–*C* (=NO_2)*C*ONH). Anal. ($C_{10}H_5F_3N_3O_3K$) calc.: C, 38.59; H, 1.62; N, 13.50; found: C, 38.92; H,1.72; N, 12.68. P_{HPLC} = 99% (mobile phase: CH_3CN/water with 0.1% trifluoroacetic acid 60/40 v/v, t_R = 16.2 min).

*5.1.3.2. 2-Nitro-3-oxo-3-[3-(trifluoromethyl)phenyl]aminopropionitrile potassium salt (**4c**).* White solid; yield 71%; m.p. 255.5–265.5 °C dec. (from H_2O); ^{1}H-NMR (DMSO-d_6): δ 7.34–8.20 (m, 4H, aromatic protons), 11.35 (br s, 1H, N*H*), ^{13}C-NMR (DMSO-d_6): δ 98.3, 115.3 (q, *C*(4), $^3J_{CF}$ 4.1 Hz), 116.8, 119.1 (q, *C*(2), $^3J_{CF}$ 3.8 Hz), 124.1 (q, *C*F$_3$, $^1J_{CF}$ 272.3 Hz), 122.8–122.9 (m), 129.4 (q, *C*(3), $^2J_{CF}$ 31.5 Hz), 129.8, 139.4, 160.4. Anal. ($C_{10}H_5F_3N_3O_3K \cdot 0.5\ H_2O$) C, H, N.

*5.1.3.3. 3-[3,5-Bis(trifluoromethyl)phenyl]amino-2-nitro-3-oxopropionitrile potassium salt (**5c**).* Pale yellow solid; yield 82%; m.p. 275.7 °C dec. (triturated with *i*Pr_2O); ^{1}H-NMR (DMSO-d_6): δ 7.68 (s, 1H, C(4)*H*), 8.40 (s, 2H, C(2)*H*), 11.47 (s, 1H, N*H*); ^{13}C-NMR (DMSO-d_6): δ 98.1, 115.3–115.4 (t, *C*(4) $^3J_{CF}$ 3.9 Hz,), 116.6, 119.3–119.4 (q, *C*(2), $^3J_{CF}$ 3.9 Hz), 123.4 (q, *C*(3), $^1J_{CF}$ 272.7 Hz), 130.5 (q, *C*(3), $^2J_{CF}$ 32.7 Hz), 140.6, 160.7. Anal. ($C_{11}H_4F_6N_3O_3K \cdot 1.65\ H_2O$) calc.: C, 32.38; H, 1.56; N, 10.30; found: C, 32.79; H, 2.09; N, 10.34. P_{HPLC} = 99% (mobile phase: CH_3CN/water with 0.1% trifluoroacetic acid 80/20 v/v, t_R = 10.6 min).

*5.1.3.4. 3-(4-Fluorophenyl)amino-2-nitro-3-oxopropionitrile potassium salt (**6c**).* Pale yellow solid; yield 89%; m.p. 265.0–266.9 °C dec. (from EtOH/*i*Pr_2O 9:1 v/v); ^{1}H-NMR (DMSO-d_6): δ 7.08–7.63 (m, 4H, aromatic protons), 11.15 (br s, 1H, N*H*); ^{13}C-NMR (DMSO-d_6): δ 98.2, 115.2 (d, *C*(3), $^2J_{CF}$ 22.1 Hz), 117.0, 120.9 (d, *C*(2), $^3J_{CF}$ 7.9 Hz), 135.0 (d, *C*(1), $^4J_{CF}$ 2.5 Hz), 157.8 (d, *C*(4), $^1J_{CF}$ 239.3 Hz), 159.9. Anal. ($C_9H_5FN_3O_3K \cdot 0.4H_2O$) C, H, N.

*5.1.3.5. 3-(3-Fluorophenyl)amino-2-nitro-3-oxopropionitrile potassium salt (**7c**).* White solid; yield 76%; m.p. 266.3–266.7 °C dec. (from H_2O); ^{1}H-NMR (DMSO-d_6): δ 6.84–7.71 (m, 4H, aromatic protons), 11.29 (s, 1H, N*H*); ^{13}C-NMR (DMSO-d_6): δ 98.3, 106.0 (d, *C*(4), $^2J_{CF}$ 26.4 Hz), 109.2 (d, *C*(2), $^2J_{CF}$ 21.2 Hz), 115.0 (d, *C*(6), $^4J_{CF}$ 2.6 Hz), 116.8, 130.2 (d, *C*(5), $^3J_{CF}$ 9.7 Hz), 140.3 (d, *C*(1), $^3J_{CF}$ 11.3 Hz), 160.1, 162.1 (d, *C*(3), $^1J_{CF}$ 241.0 Hz). Anal. ($C_9H_5FN_3O_3K$) C, H, N.

*5.1.3.6. 3-(2-Fluorophenyl)amino-2-nitro-3-oxopropionitrile potassium salt (**8c**).* Pale yellow solid, yield 80%; m.p. 262.7–263.2 °C dec. (triturated with *i*Pr_2O); ^{1}H-NMR (DMSO-d_6): δ 7.05–7.40 (m, 3H, aromatic protons), 8.35–8.63 (m, 1H, C(3)*H*), 11.65 (s, 1H, N*H*); ^{13}C-NMR (DMSO-d_6): δ 98.5, 114.8 (d, *C*(3), $^2J_{CF}$ 19.0 Hz), 116.7, 120.6 (d, *C*(5), $^4J_{CF}$ 1.6 Hz), 123.0 (d, *C*(4), $^3J_{CF}$ 7.6 Hz), 124.5 (d, *C*(6), $^3J_{CF}$ 3.5 Hz), 150.3, 151.6 (d, *C*(2), $^1J_{CF}$ 241.7 Hz), 159.8. Anal. ($C_9H_5FN_3O_3K \cdot 0.1H_2O$) C, H, N.

*5.1.3.7. 3-(3,5-Difluorophenyl)amino-2-nitro-3-oxopropionitrile potassium salt (**9c**).* White solid; yield 87%; m.p. 267.4–268.9 °C dec. (from H_2O); ^{1}H-NMR (DMSO-d_6): δ 6.81–7.46 (m, 4H, aromatic protons), 11.31 (s, 1H, N*H*); ^{13}C-NMR (DMSO-d_6) δ 98.4, 98.7 (t, *C*(4), $^2J_{CF}$ 26.3 Hz), 102.9–103.3 (m, *C*(2)), 117.6, 142.1 (t, *C*(1), $^3J_{CF}$ 14.1 Hz), 161.3, 163.3 (dd, *C*(3), $^1J_{CF}$ 242.5 Hz, $^3J_{CF}$ 15.5 Hz). Anal. ($C_9H_4F_2N_3O_3K$) calc.: C, 38.71; H, 1.44; N, 15.05; found: C, 39.19; H, 2.11; N, 14.23. P_{HPLC} = 98% (mobile phase: CH_3CN/water with 0.1% trifluoroacetic acid 60/40 v/v, t_R = 13.7 min).

*5.1.3.8. 2-Nitro-3-(4-nitrophenyl)amino-3-oxopropionitrile potassium salt (**10c**).* Yellow solid; yield 68%; m.p. 252.8–253.6 °C dec. (triturated with isopropyl ether); ^{1}H-NMR (DMSO-d_6): δ 7.86–8.20 (m, 4H, aromatic protons), 11.59 (s, 1H, N*H*); ^{13}C-NMR (DMSO-d_6): δ 98.5, 116.5, 118.8, 124.9, 141.8, 144.8, 160.3. Anal. ($C_9H_5N_4O_5K$) C, H, N.

*5.1.3.9. 3-(4-Methylphenyl)amino-2-nitro-3-oxo-propionitrile potassium salt (**12c**).* Pale yellow solid; yield 50%; m.p. 277.2–277.3 °C dec. (triturated with *i*Pr_2O); ^{1}H-NMR (DMSO-d_6): δ 2.27 (s, 3H, *C*H_3), 7.07–7.46 (m, 4H, aromatic protons), 11.10 (s, 1H, N*H*); ^{13}C-NMR (DMSO-d_6): δ 21.3, 106.1, 118.0, 120.0, 130.1, 132.7, 137.0, 160.7. Anal. ($C_{10}H_8N_3O_3K$) C, H, N.

*5.1.3.10. 2-Nitro-3-oxo-3-(biphenyl-4-yl)aminopropionitrile potassium salt (**14c**).* Yellow solid; yield 20%; m.p. 269.1–271.7 °C dec. (triturated with *i*Pr_2O); ^{1}H-NMR (DMSO-d_6): δ 7.29–7.70 (m, 9H, aromatic protons), 11.27 (s, 1H, N*H*); ^{13}C-NMR (DMSO-d_6): δ 110.0, 117.9, 120.4, 127.1, 127.8, 127.9, 129.8, 135.4, 139.0, 140.8, 160.9. Anal. ($C_{15}H_{10}N_3O_3K$) C, H, N.

*5.2. X-ray structure determination of **6b** and **8b***

Crystal and refinement data are reported in Table 4. The reflection data, using a crystal obtained from toluene solution, have been collected on a Gemini R Ultra diffractometer [25]. The hydrogen atom coordinates have been calculated (**6b**) or found (**8b**) and refined with U_{iso} set at 1.5 times U_{eq} of the corresponding atom (**6b**) or with U_{iso} free (**8b**). All other atoms have been anisotropically refined. Programs used were CrysAlisPro [25] for data collection and correction and SHELXTL [26] for structure solution, refinement and molecular graphics. No absorption correction has been made. CIF files have been deposited at the Cambridge Crystallographic Data Centre as CCDC 784463 for **6b** and CCDC 784464 for **8b**; bond length and angles are reported in the Supplementary Material.

5.3. Evaluation of stability in aqueous buffer solutions

A solution of each compound (10 mM) in methanol was added to phosphate buffer (pH 7.4, 50 mM) preheated at 37 °C. To carry out the assay at pH 1 and pH 10, 0.1 M HCl and 0.1 M phosphate buffer were used, respectively. The final concentration of the compound was 100 μM. The resulting solution was maintained at 37.0 ± 0.5 °C, and at 30-min time intervals the reaction mixture was

Table 4
Crystal data and refinement parameters for compounds **6b** and **8b**.

Compd	**6b**	**8b**
Empirical formula	$C_9H_6FN_3O_2$	$C_9H_6FN_3O_2$
Formula weight	207.17	207.17
Temperature	293(2) K	293(2) K
Wavelength	0.71073 Å	0.71073 Å
Crystal system, space group	Monoclinic, Pn	Monoclinic, $P2_1/c$
Unit cell dimensions	$a = 13.3757(6)$ Å $b = 4.8077(2)$ Å $c = 15.0160(6)$ Å $\beta = 103.704(3)^\circ$	$a = 7.4210(4)$ Å $b = 11.0620(4)$ Å $c = 11.2802(3)$ Å $\beta = 96.658(3)^\circ$
Volume	938.14(7) Å^3	919.76(6) Å^3
Z, Calculated density	4, 1.467 g cm^{-3}	4, 1.496 g cm^{-3}
Absorption coefficient	0.120 mm^{-1}	0.123 mm^{-1}
$F(000)$	424	424
Theta range for data collection	3.14–32.69°	3.32–32.67°
Limiting indices	$-20 \le h \le 15$, $-6 \le k \le 7$, $-22 \le l \le 19$	$-8 \le h \le 10$, $-14 \le k \le 16$, $-17 \le l \le 16$
Reflections collected/unique	11,621/4286 [R(int) = 0.0510]	12,027/3132 [R(int) = 0.0534]
Completeness to theta = 32.69	93.5%	92.7%
Refinement method	Full-matrix least-squares on F^2	Full-matrix least-squares on F^2
Data/restraints/parameters	4286/2/271	3132/0/160
Goodness-of-fit on F^2	0.894	0.798
Final R indices [$I > 2$sigma(I)]	$R_1 = 0.0878$, w$R_2 = 0.2025$	$R_1 = 0.0405$, w$R_2 = 0.0847$
R indices (all data)	$R_1 = 0.1757$, w$R_2 = 0.2413$	$R_1 = 0.1407$, w$R_2 = 0.0990$
Max. and min. electron density	0.731 and −0.279 e Å^{-3}	0.136 and −0.161 e Å^{-3}

analyzed by RP-HPLC. Incubations were conducted in triplicate. The RP-HPLC procedure allowed the separation and quantitation of the unchanged compound and newly formed oxime derivatives. HPLC analyses were performed with the HP1100 chromatograph system previously described. The analytical column was a Zorbax Eclipse XDB-C8 (Agilent, 150 × 4.6 mm, 5 μm particle size). The mobile phase consisted of methanol/water with 0.1% trifluoroacetic acid (ranging from 60/40 to 75/25 ratio, according to the retention factor of the compounds); flow rate and injection volume were 1.2 mL min^{-1} and 20 μL, respectively. The column effluent was monitored at 230 and 270 nm referenced against a 360 nm wavelength. Quantitation was performed by comparison of peak areas with standards chromatographed under the same conditions. The percentage of unchanged compound versus time was fitted with a one-phase exponential decay equation using GraphPad Prism version 5 to obtain k_{obs}; $t_{1/2}$ was calculated from Eq. (1):

$$t_{1/2} = 0.693/k_{obs} \quad (1)$$

5.4. Dissociation constant determination

Potentiometric titrations were performed using the GLpK_a apparatus (Sirius Analytical Instruments Ltd., Forest Row, East Sussex, UK). Because of their low aqueous solubility all the compounds required titrations in the presence of methanol as cosolvent: at least five different hydro-organic solutions (ionic strength adjusted to 0.15 M with KCl) of the compounds (20 mL, about 1 mM in 24–58 wt% methanol) were initially acidified to pH 1.8 with 0.5 N HCl; the solutions were then titrated with standardized 0.5 N KOH to pH 10.5. The initial estimates of the p$_s K_a$ values (the apparent ionization constants in the water–methanol mixtures) were obtained and aqueous pK_a values were determined by extrapolation to zero content of cosolvent according to the Yasuda–Shedlovsky procedure [16]. All titrations were performed under N_2 at 25.0 ± 0.1 °C.

5.5. Biological evaluation

5.5.1. Preparation of rat liver membranes

Crude mitochondrial/microsomal membranes from livers of male Wistar rats (200–250 g) were prepared by homogenisation and differential centrifugation [20,27]. Homogenisation buffer was 25 mM sodium phosphate, 250 mM sucrose and 0.3% v/v Protease Inhibitor Cocktail for use with mammalian cell and tissue extracts (SIGMA Catalog Number: P8340) at pH 7.4. The homogenate (9 mL homogenisation buffer/g wet tissue) was centrifuged at 470*g* for 10 min, the supernatant retained, and the pellets re-homogenised in buffer (4.5 mL/g wet tissue). This homogenate was centrifuged (470*g*, 10 min) and the supernatant was combined with the one obtained earlier and centrifuged (50,000*g*, 60 min). The membranes were washed by resuspension in homogenisation buffer plus 150 mM NaCl, 1 mM EDTA and 1 mM EGTA before final centrifugation (50,000*g*, 60 min) and re-suspension in the homogenisation buffer (2 mL/g wet tissue). All of the above steps were performed at 4 °C and aliquots of the final membrane preparation were stored at −80 °C.

5.5.2. Dihydroorotate dehydrogenase assay

Inhibition of rat liver DHODH activity by tested compounds was assessed using a DCIP-linked assay. Membranes (0.8 mg protein mL^{-1}) were incubated at 37 °C in 50 mM Tris–HCl, 0.1% Triton X-100, 1 mM KCN, pH 8.0 with coenzyme Q_{10} (100 μM) and the tested compounds at different concentrations (final DMSO 0.1% v/v). The reaction was initiated by addition of DHO (500 μM), and the reduction of DCIP (50 μM) was monitored by the decrease in absorbance at 650 nm. The initial rate of the enzyme reaction, in the presence and in the absence of potential inhibitor, was measured in the first five minutes ($\epsilon = 10{,}400$ M^{-1} cm^{-1} in our experimental conditions) and a preliminary IC_{50} value was calculated, when possible, according to Eq. (2) [28]:

$$v = V/(1 + [I]/IC_{50}) \quad (2)$$

where [I] is the inhibitor concentration.

Michaelis–Menten constant (K_m) for DHO, determined by the usual procedure, was found to be 14.6 μM, in keeping with previous work [28].

5.6. Molecular modelling

The molecular models of compounds **3b**, **3c**, **10b**, **10c**, **14b**, **14c** and orotate were built using standard bond lengths and angles with the MOE software suite [29]. In accordance with their pK_a values (Table 3), all compounds were modelled as anions; their geometries were optimized with the Newton–Raphson method (MMFF94s force field, GB/SA implicit solvent model) until the gradient was lower than 0.001 kcal mol^{-1} Å^{-1}. A Monte Carlo conformational search was carried out with the ConfSearch module implemented in MOE. The most stable conformers were then subjected to further optimization by an ab initio HF/6-31G(d) method using GAMESS-US [30]. The experimental crystallographic structures of human DHODH in complex with **1a** (PDB ID 1D3H) as well as of rat DHODH in complex with brequinar (PDB ID 1UUO) were retrieved from the Protein Data Bank [31]. The coordinates of a few second-shell residues surrounding the active site (70–72 in 1D3H, 70–73 in 1UUO) were missing and were modelled with the Homology module implemented in MOE. Missing hydrogen atoms

were added to both enzymes in standard positions, then their coordinates were optimized with the SANDER module of the AMBER 10 software package [32], while harmonically restraining heavy atoms to the initial crystallographic coordinates with a force constant of 1000 kcal mol^{-1} Å^{-2}. AMBER FF99 parameters were assigned to protein atoms and GAFF parameters to the co-crystallized inhibitor and orotate, while atom-centred point charges were fitted to the quantum-mechanical electrostatic potential according to the RESP method [33]. Equilibrium internal coordinates, force-field parameters and electrostatic charges for the FMN cofactor were taken from literature [34]. After removing the co-crystallized inhibitor, docking of compounds **3b**, **3c**, **10b**, **10c**, **14b**, **14c** was carried out using AutoDock 4.0.1 [35–37]. A grid with a 0.375 Å step size was centred on the inhibitor binding site and energy maps were pre-computed with AutoGrid, then flexible docking was carried out with AutoDock. The target proteins were kept rigid, while ligands were left free to explore the conformational space inside the enzyme cavity; 200 separate docking simulations were run on each target using the Lamarckian genetic algorithm with default parameters.

The geometries of the most stable conformer of both *E* and *Z* isomers of compounds **3b**, **10b**, **14b** were optimized with a DFT method at the RB3LYP/6-31G(*d*) level of theory. Single point energy calculations at the RB3LYP/6-311G(2*d*,2*p*) level were then carried out to compute the relative stabilities of the two isomers. For compound **3b** the minimum energy reaction path for the *E-Z* isomerisation was computed as previously described [14] by constraining the C-N-O angle at 33 intermediate values with the same RB3LYP/6-31G(*d*)//RB3LYP/6-311G(2*d*,2*p*) DFT method used for ground state geometries. Frequency calculations were performed at the same level of theory as the geometry optimizations to obtain zero-point energies (no scaling) and to characterize the stationary points as local minima, or as a first-order saddle point for the transition state structure in the isomerisation of **3b**.

Acknowledgements

This work was supported by a grant from Regione Piemonte Progetto Ricerca Sanitaria Finalizzata 2009.

Appendix. Supplementary material

Supplementary data associated with this article can be found in the online version, at doi:10.1016/j.ejmech.2010.10.029.

References

[1] A.M. Krensky, F. Vincenti, Immunosuppressants, tolerogens and immunostimulants. in: L.L. Brunton, J.S. Lazo, K.L. Parker (Eds.), Goodman & Gilman's The Pharmacological Basis of Therapeutics. Mc Graw-Hill, New York, 2006, pp. 1405–1432.

[2] (a) H.T. Silva Jr., R.E. Morris, Leflunomide and malononitrilamides, Am. J. Med. Sci. 313 (1997) 289–301;
(b) C. Papageorgiou, M. Zurini, H.P. Weber, X. Borer, Leflunomide's bioactive metabolite has the minimal structural requirements for the efficient inhibition of human dihydroorotate dehydrogenase, Bioorg. Chem. 25 (1997) 233–238;
(c) C. Papageorgiou, K. Akyel, X. Borer, L. Oberer, G. Rihs, 3-Hydroxy-2-cyanoalk-2-enamides, and 2-cyano-2-(tetrahydrofuran-2-ylidene)- and 2-cyano-2-(tetrahydropyran-2-ylidene)acetamides: synthesis, structure, and solvent-dependent (Z)/(E)-isomerism, Helv. Chim. Acta 81 (1998) 1319–1328;
(d) G. Bertolini, M. Aquino, M. Biffi, G. d'Atri, F. Di Pierro, F. Ferrario, P. Mascagni, F. Somenzi, A. Zaliani, F. Leoni, A new rational hypothesis for the pharmacophore of the active metabolite of leflunomide, a potent immunosuppressive drug, J. Med. Chem. 40 (1997) 2011–2016;
(e) R.I. Fox, M.L. Herrmann, C.G. Frangou, G.M. Wahl, R.E. Morris, V. Strand, B.J. Kirschbaum, Mechanism of action for leflunomide in rheumatoid arthritis, Clin. Immunol. 93 (1999) 198–208.

[3] (a) P. Pino, A. Scartabelli, E. Lombardi, Rend. Istit. Lombardo Sci. Lettere 87 (1954) 229–246;
(b) T.L. Gilchrist, Ring-opening of five-membered heteroaromatic anions, Adv. Heterocycl. Chem. 41 (1987) 41–74.

[4] A.S. Kalgutkar, H.T. Nguyen, A.D.N. Vaz, A. Doan, D.K. Dalvie, D.G. McLeod, J.C. Murray, In vitro metabolism studies on the isoxazole ring scission in the anti-inflammatory agent leflunomide to its active α-cyanoenol metabolite A771726: mechanistic similarities with the cytochrome P450-catalyzed dehydration of aldoximes, Drug Metab. Dispos. 31 (2003) 1240–1250.

[5] J.P. Davis, G.A. Cain, W.J. Pitts, R.L. Magolda, R.A. Copeland, The immunosuppressive metabolite of leflunomide is a potent inhibitor of human dihydroorotate dehydrogenase, Biochemistry 35 (1996) 1270–1273.

[6] R.R. Bartlett, H. Anagnostopulos, T. Zielinski, T. Mattar, R. Schleyerbach, Effects of leflunomide on immune responses and models of inflammation, Semin. Immunopathol. 14 (1993) 381–394.

[7] T. Mattar, K. Kochhar, R. Bartlett, E.G. Bremer, A. Finnegan, Inhibition of the epidermal growth factor receptor tyrosine kinase activity by leflunomide, FEBS Lett. 334 (1993) 161–164.

[8] A. De Munno, V. Bertini, A. Menconi, G. Denti, Su alcuni derivati del 3-fenil-1,2,5-oxadiazolo, Atti Soc. Tosc. Sci. Nat. Mem. (1975) 334–342.

[9] A. Olofson, J.S. Michelman, Furazan, J. Org. Chem. 30 (1965) 1854–1859.

[10] A.B. Sheremetev, N.N. Makhova, W. Friedrichsen, Monocyclic furazans and furoxans, Adv. Heterocycl. Chem. 78 (2001) 65–188.

[11] D. Eddings, C. Barnes, N. Gerasimchuk, P. Durham, K. Domasevich, First bivalent palladium and platinum cyanoximates: synthesis, characterization, and biological activity, Inorg. Chem. 43 (2004) 3894–3909.

[12] G.C. Levy, G.L. Nelson, Carbon-13 NMR study of aliphatic amides and oximes. Spin-lattice relaxation times and fast internal motions, J. Am. Chem. Soc. 94 (1972) 4897–4901.

[13] N. Gerasimchuk, T. Maher, P. Durham, K.V. Domasevitch, J. Wilking, A. Mokhir, Tin(IV) cyanoximates: synthesis, characterization, and cytotoxicity, Inorg. Chem. 46 (2007) 7268–7284.

[14] J. Gálvez, A. Guirado, A theoretical study of topomerization of imine systems: inversion, rotation or mixed mechanisms? J. Comput. Chem. 31 (2010) 520–531.

[15] F.H. Allen, O. Kennard, D.G. Watson, L. Brammer, A.G. Orpen, R. Taylor, Tables of bond lengths determined by X-ray and neutron diffraction Part 1. Bond lengths in organic compounds, J. Chem. Soc., Perkin Trans. 2 (1987) S1–S19.

[16] A. Avdeef, J.E.A. Comer, S.J. Thomson, pH-Metric log P. 3. Glass electrode calibration in methanol-water, applied to pK_a determination of water-insoluble substances, Anal. Chem. 65 (1993) 42–49.

[17] M.E. Jones, Pyrimidine nucleotide biosynthesis in animals: genes, enzymes, and regulation of UMP biosynthesis, Annu. Rev. Biochem. 49 (1980) 253–279.

[18] S. Liu, E.A. Neidhardt, T.H. Grossman, T. Ocain, J. Clardy, Structures of human dihydroorotate dehydrogenase in complex with antiproliferative agents, Structure 8 (2000) 25–33.

[19] E.A. Kuo, P.T. Hambleton, D.P. Kay, P.L. Evans, S.S. Matharu, E. Little, N. McDowall, C.B. Jones, C.J.R. Hedgecock, C.M. Yea, A.W.E. Chan, P.W. Hairsine, I.R. Ager, W.R. Tully, R.A. Williamson, R. Westwood, Synthesis, structure–activity relationships, and pharmacokinetic properties of dihydroorotate dehydrogenase inhibitors: 2-cyano-3-cyclopropyl-3-hydroxy- *N*-[3′-methyl-4′-(trifluoromethyl)phenyl]propenamide and related compounds, J. Med. Chem. 39 (1996) 4608–4621.

[20] R.A. Williamson, C.M. Yea, P.A. Robson, A.P. Curnock, S. Gadher, A.B. Hambleton, K. Woodward, J.M. Bruneau, P. Hambleton, D. Moss, T.A. Thomson, S. Spinella-Jaegle, P. Morand, O. Courtin, C. Sautes, R. Westwood, T. Hercend, E.A. Kuo, E. Ruuth, Dihydroorotate dehydrogenase is a high affinity binding protein for A771726 and mediator of a range of biological effects of the immunomodulatory compound, J. Biol. Chem. 270 (1995) 22,467–22,472.

[21] M. Hansen, J. Le Nours, E. Johansson, T. Antal, A. Ullrich, M. Loffler, S. Larsen, Inhibitor binding in a class 2 dihydroorotate dehydrogenase causes variations in the membrane-associated *N*-terminal domain, Protein Sci. 13 (2004) 1031–1042.

[22] A. Ramakrishnan, K. Gobind, K. Neeraj, S. Dnyaneshwar, An improved process for preparation of Leflunomide, Intl. Appl. No.: PCT/IN2006/000359.

[23] Y.A. Strelenko, A.B. Sheremetev, L.I. Khmel'nitskii, Monosubstituted furazans. I. NMR investigation, Chem. Heterocycl. Comp 28 (1992) 927–930.

[24] Y.Yu. Morzherin, M.Yu. Kolobov, V.S. Mokrushin, M. Brauer, E. Anders, V.A. Bakulev, Heterocyclization of compounds containing diazo and cyano groups. Part 6. Theoretical and experimental investigations of cyclization of 2-cyano-2-diazoacetamides to 5-hydroxy-1,2,3-triazole-4-carbonitriles, Chem. Heterocycl. Comp. 36 (2000) 22–36.

[25] CrysAlisPro, Oxford Diffraction Ltd., Yarnton, UK.

[26] SHELXTL Version 5.1, Bruker AXS Inc., Madison, WI, USA.

[27] R.A. Williamson, P.G. Strange, Evidence for the importance of a carboxyl group in the binding of ligands to the D_2 dopamine receptor, J. Neurochem. 55 (1990) 1357–1365.

[28] A. Ullrich, W. Knecht, M. Fries, M. Loffler, Recombinant expression of *N*-terminal truncated mutants of the membrane bound mouse, rat and human flavoenzyme dihydroorotate dehydrogenase: a versatile tool to rate inhibitor effects? Eur. J. Biochem. 268 (2001) 1861–1868.

[29] MOE Version 2009.10. Chemical Computing Group Inc., Montreal, Quebec, Canada, 2009.

[30] M.W. Schmidt, K.K. Baldridge, J.A. Boatz, S.T. Elbert, M.S. Gordon, J.H. Jensen, S. Koseki, N. Matsunaga, K.A. Nguyen, S.J. Su, T.L. Windus, M. Dupuis, J.A. Montgomery, General atomic and molecular electronic structure system, J. Comput. Chem. 14 (1993) 1347–1363.

[31] The RCSB Protein Data Bank, Available from: http://www.rcsb.org/ (last accessed 25 October 2010).
[32] D.A. Case, T.A. Darden, T.E. Cheatham III, C.L. Simmerling, J. Wang, R.E. Duke, R. Luo, M. Crowley, R.C. Walker, W. Zhang, K.M. Merz, B. Wang, S. Hayik, A. Roitberg, G. Seabra, I. Kolossvary, K.F. Wong, F. Paesani, J. Vanicek, X. Wu, S.R. Brozell, T. Steinbrecher, H. Gohlke, L. Yang, C. Tan, J. Mongan, V. Hornak, G. Cui, D.H. Mathews, M.G. Seetin, C. Sagui, V. Babin, P.A. Kollman, AMBER 10. University of California, San Francisco (USA), 2008.
[33] J. Wang, P. Cieplak, P.A. Kollman, How well does a restrained electrostatic potential (RESP) model perform in calculating conformational energies of organic and biological molecules? J. Comput. Chem. 21 (2000) 1049–1074.
[34] C. Schneider, J. Sühnel, A molecular dynamics simulation of the flavin mononucleotide–RNA aptamer complex, Biopolymers 50 (1999) 287–302.
[35] D.S. Goodsell, A.J. Olson, Automated docking of substrates to proteins by simulated annealing, Proteins Struct. Funct. Bioinf. 8 (1990) 195–202.
[36] G.M. Morris, D.S. Goodsell, R. Huey, A.J. Olson, Distributed automated docking of flexible ligands to proteins: parallel applications of AutoDock 2.4, J. Comput. Aided Mol. Des. 10 (1996) 293–304.
[37] G.M. Morris, D.S. Goodsell, R.S. Halliday, R. Huey, W.E. Hart, R.K. Belew, A.J. Olson, Automated docking using a Lamarckian genetic algorithm and an empirical binding free energy function, J. Comput. Chem. 19 (1998) 1639–1662.